Soft Matter

PAPER

View Article Online
View Journal | View Issue

CrossMark click for updates

Cite this: *Soft Matter*, 2015, **11**, 889

Non-additive simple potentials for pre-programmed self-assembly

Daniel Salgado-Blanco and Carlos I. Mendoza*

A major goal in nanoscience and nanotechnology is the self-assembly of any desired complex structure with a system of particles interacting through simple potentials. To achieve this objective, intense experimental and theoretical efforts are currently concentrated in the development of the so-called "patchy" particles. Here we follow a completely different approach and introduce a very accessible model to produce a large variety of pre-programmed two-dimensional (2D) complex structures. Our model consists of a binary mixture of particles that interact through isotropic interactions that enable them to self-assemble into targeted lattices by the appropriate choice of a small number of geometrical parameters and interaction strengths. We study the system using Monte Carlo computer simulations and, despite its simplicity, we are able to self-assemble potentially useful structures such as chains, stripes, and Kagomé, twisted Kagomé, honeycomb, square, Archimedean and quasicrystalline tilings. Our model is designed in such a way that it may be implemented using discotic particles or, alternatively, using exclusively spherical particles interacting isotropically. Thus, it represents a promising strategy for bottom-up nano-fabrication.

Received 4th November 2014
Accepted 27th November 2014

DOI: 10.1039/c4sm02436b

www.rsc.org/softmatter

Published on 28 November 2014. Downloaded by FAC DE QUIMICA on 03/03/2016 17:58:19.

Introduction

The quest for new materials with unusual physical properties and the need to produce devices of technological interest at the nanoscale have boosted the design of new methods for the fabrication of complex colloidal nanostructures. Processes such as micro- and nano-fabrication are time consuming and prohibitively expensive; therefore they are difficult to apply below a certain length scale.[1] As a result, the search for building blocks on the mesoscopic scales that self-organize into potentially useful structures by virtue of their mutual interactions and shape is extremely important. One of the main challenges is the ability to program the properties of the individual components so that they organize into a desired structure.[2] In many cases this objective is pursued by trying to emulate the self-assembly of living systems. Since most biomolecular objects interact through directionally specific forces, a large amount of work has been done to mimic the anisotropic nature of these interactions,[3–5] specifically, with the design and use of patchy[6–8] and Janus[9–12] particles. This approach captures much of the richness of nature's self-assembled structures and has been successful in building some types of lattices.[13] However, the production of particles with controlled patchiness in the laboratory is still largely unavailable, although there has been impressive progress in their synthesis.[5]

Particles interacting through simple isotropic interactions of the core–corona type are also able to self-assemble in a large variety of structures.[14,15] However, in general, it is difficult to predict which kind of structures can be obtained from these potentials and an exploration of the parameter space has to be performed to identify the different regions of the phase space where a resulting structure appears. In order to circumvent this difficulty, different, mainly theoretical, procedures have been devised. These are the so-called inverse optimization techniques which consist in determining the kind of isotropic interaction potential that would result in the self-assembly of a desired structure.[16,17] Although this procedure has great potential, to date, it results in very complex interactions difficult to translate into a realistic system. Multi-component colloidal systems interacting through simpler isotropic potentials[18–21] are also an alternative to build complex lattices.

In this work we propose a non-additive purely isotropic interaction in a binary mixture of particles that can lead to a large variety of different desired structures. Of particular interest is the formation of nanometer-length-scale patterns in two dimensions due to their potential in many applications, such as optics, photonics, sensing and others.[12] Among the patterns that are being pursued, we can highlight the square lattice whose symmetry is appropriate for use in nanocircuitry and therefore with prospects in the electronic industry,[18] the Kagomé lattice for its applications in the study of frustrated magnetism,[22–24] or the unusual mechanical properties like the auxetic response of the twisted Kagomé lattices,[25] the honeycomb lattice for its electronic properties motivated by its three-

Instituto de Investigaciones en Materiales, Universidad Nacional Autónoma de México, Apdo. Postal 70-360, 04510 México, D.F., Mexico. E-mail: cmendoza@iim.unam.mx

Published on 28 November 2014. Downloaded by FAC DE QUIMICA on 03/03/2016 17:58:19.

dimensional analog, the diamond lattice,[16] and the quasicrystals for photonic applications[26] among others. With our model we are able to self-assemble an enormous variety of useful structures in 2D, among others, chains, stripes, and Kagomé, twisted Kagomé, honeycomb, square, Archimedean and quasicrystalline lattices. Recently, a non-additive system in three dimensions has been used to construct a tetrahedral network glass former.[27] However, to the best of our knowledge, a systematic application of this kind of models to produce a large variety of pre-defined structures has not been carried out.

Although our study is numerical, we believe that the model should be feasible in practice due to the simple shape of the particles involved and the possibility of decorating their surface with double-stranded DNA or other well established methods to produce short range interactions. Furthermore, it is possible to mimic the system with a setup consisting of a cell containing a binary mixture of spherical particles interacting isotropically, thus bypassing the need to fabricate particles with complicated shapes and interactions. An experimental setup somewhat similar to that proposed in this work has been used to emulate core-softened colloids.[28]

Model

Our system consists of a non-additive binary mixture of particles as depicted in Fig. 1a. In a two-component mixture normally the distance of closest approach between hard particles of different species is a simple mean of the diameters of the particles of each species. The non-additive hard particle mixture generalizes this so that this distance can be smaller or larger than the arithmetic mean of the like-species diameters.[29,30] A 2D version of our model can be achieved as follows: one species consists of two coupled layers of attractive hard discs as shown by the mushroom-shaped particles (M) in Fig. 1a. The second species consists of attractive hard discs (D) and both species are able to move only in the plane perpendicular to their symmetry axis. The interaction between particles is represented by an axially symmetric pair potential $V(r)$ composed of an impenetrable core surrounded by an adjacent square well. Our model is designed to produce two-dimensional self-assembled structures in which M-type particles are surrounded by discs in such a way that each type of particles arranges in mutually intercalated lattices. This methodology is particularly useful for the self-assembly of open lattices. Since the lattices of the two species are mutually intercalated, the open space of a given lattice can be occupied by a particle of the second species, thus providing stability to the structure during the formation process. Discs have a core of diameter σ_0 and a thin square-well potential with range $\lambda_0\sigma_0$. The interaction between mushroom-shaped particles is represented by a core of diameter σ_2 and a thin square-well potential with range $\lambda_2\sigma_2$. Finally, the interaction between a mushroom-shaped particle and a disc consists of a hard core with diameter $\sigma_{01} = (\sigma_0 + \sigma_1)/2$ and a thin adjacent square-well potential with range $\lambda_{01}\sigma_{01}$. The non-additive nature of the model means that $\sigma_{01} = (\sigma_0 + \sigma_1)/2 = (1 + \Delta)(\sigma_0 + \sigma_2)/2$, with $\Delta = (\sigma_1 - \sigma_2)/(\sigma_0 + \sigma_2)$. The value of Δ in our model is always negative ($-1 < \Delta \leq 0$) which means that the distance of closest approach between a disc and a M-type particle is smaller than the mean of the diameters of the particles of each species. The interaction potentials are also depicted in Fig. 1a, where ε_0, ε_2, and ε_{01} are depths of the potential wells. Mathematically, the interaction potentials can be expressed by the following set of equations

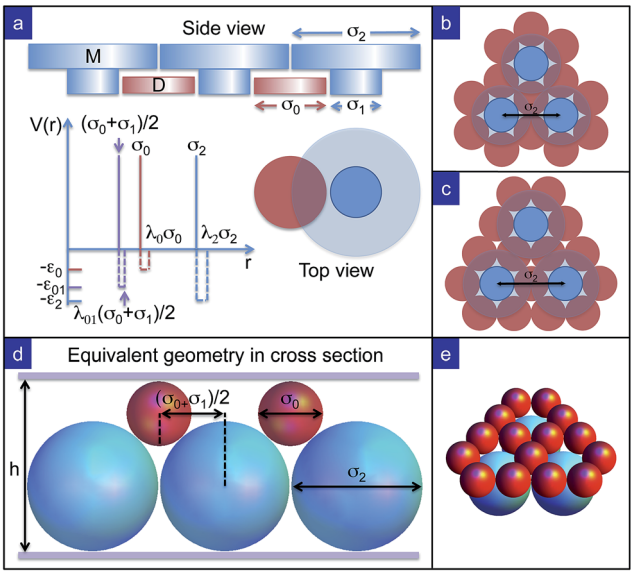

Fig. 1 Description of the model. (a) Binary mixture of mushroom-shaped particles M (blue particles) and discs D (red particles). The interaction potential between the hard discs is depicted by the red line, the interaction between mushroom-shaped particles is depicted by the blue line, and finally, the interaction between a disk and a mushroom-shaped particle is depicted by the purple line. The narrow attractive square well potential at the surface of the particles is indicated by dashed lines. (b) and (c) Schematic representation of two different lattices obtained for the same value $\sigma_1/\sigma_0 = 1$. In both cases M-type particles lie in a triangular lattice; however, in panel (b) the discs form a honeycomb lattice for $\sigma_2/\sigma_0 = \sqrt{3}$ while in panel (c) they form a Kagomé lattice for $\sigma_2/\sigma_0 = 2$. (d) Realization of the model using exclusively spherical particles interacting isotropically that are immersed in a cell of thickness h. Large spheres (blue) lie at the bottom of the cell and the small spheres (red) are located at the top of the cell. The non-additive parameter σ_1/σ_0 can be controlled changing the thickness of the cell h. (e) Schematic representation of the lattice obtained using the setup (d) and with the same parameters used to obtain the lattice of panel (c).

$$V_{DD}(r) = \begin{cases} \infty, & \text{if } r \leq \sigma_0 \\ -\varepsilon_0, & \text{if } \sigma_0 < r \leq \lambda_0\sigma_0, \\ 0, & \text{if } r > \lambda_0\sigma_0 \end{cases}$$

$$V_{MM}(r) = \begin{cases} \infty, & \text{if } r \leq \sigma_2 \\ -\varepsilon_2, & \text{if } \sigma_2 < r \leq \lambda_2\sigma_2, \\ 0, & \text{if } r > \lambda_2\sigma_2 \end{cases}$$

$$V_{DM}(r) = \begin{cases} \infty, & \text{if } r \leq \dfrac{(\sigma_0 + \sigma_1)}{2} \\ -\varepsilon_{01}, & \text{if } \dfrac{(\sigma_0 + \sigma_1)}{2} < r \leq \lambda_{01}\dfrac{(\sigma_0 + \sigma_1)}{2}, \\ 0, & \text{if } r > \lambda_{01}\dfrac{(\sigma_0 + \sigma_1)}{2} \end{cases}$$

This journal is © The Royal Society of Chemistry 2015

Published on 28 November 2014. Downloaded by FAC DE QUIMICA on 03/03/2016 17:58:19.

where V_{ij} represents the interaction potential between a particle i = D, M and a particle j = D, M. The distance between the central axes of the particles is r.

We study our system through Monte Carlo (MC) simulations at a constant number of particles N, volume V, and temperature T (NVT simulations). Our objective is to assemble different kinds of pre-programmed structures in 2D, specifically, lattices with different symmetries that are relevant for their scientific or technological interest. The simplest lattice to assemble in 2D is the regular triangular lattice. More difficult to assemble are open structures since they do not maximize the translational entropy of the particles.[24] In our model M-type particles are used as a tool to produce open lattices made of discs and vice versa. Among the many possible choices for the geometrical parameters, one interesting possibility is to consider that each M-type particle is surrounded by n discs ($n \geq 3$) closely packed around the central M-type particle due to the attractive interaction $V_{DM}(r)$. The value of σ_1 needed to allocate the discs is given by

$$\frac{\sigma_1}{\sigma_0} = \frac{\sqrt{2\left[1+\cos\left(\frac{2\pi}{n}\right)\right]}}{\sin\left(\frac{2\pi}{n}\right)} - 1 = \csc\left(\frac{\pi}{n}\right) - 1. \quad (1)$$

A given M-type particle may or may not share its surrounding discs with other M-type particles. The way the discs are shared will be determined by the value taken by σ_2 to finally produce the desired lattice. For instance, in the tiling depicted in Fig. 1b where $n = 6$, the value σ_2 is chosen so that each M-type particle shares two discs with each of its neighboring M-type particles. On the other hand, in Fig. 1c, even if each M-type particle is again surrounded by six discs, the value chosen for σ_2 is such that each M-type particle shares only one disc with each of its neighboring M-type particles. Lattices similar to the one shown in Fig. 1b, with each M-type particle surrounded by n discs sharing two of them with a neighboring M-type particle, can be constructed by choosing

$$\frac{\sigma_2}{\sigma_0} = \sqrt{\frac{\sigma_1}{\sigma_0}\left(2+\frac{\sigma_1}{\sigma_0}\right)} = \cot\left(\frac{\pi}{n}\right). \quad (2)$$

Steric interactions between discs restrict the use of eqn (2) to $n \leq 12$.

On the other hand, for lattices similar to the one shown in Fig. 1c, in which a M-type particle shares only one disc with a neighboring M-type particle

$$\frac{\sigma_2}{\sigma_0} = 1 + \frac{\sigma_1}{\sigma_0} = \csc\left(\frac{\pi}{n}\right). \quad (3)$$

Steric interactions between discs restrict the use of eqn (3) to $n \leq 6$.

Sometimes it is energetically more favorable for the system to phase separate. To suppress this behavior, suitable values for the potential wells should be chosen so that the discs prefer to stick around a M-type particle.

Thus, the model can form a large variety of target structures by simply tailoring the geometrical parameters σ_1/σ_0, and σ_2/σ_0, and strengths of the potential wells ε_0, ε_2, and ε_{01}. Widths of the potential wells λ_0, λ_2, and λ_{01} do not significantly alter obtained lattices and are only used for fine tuning the resulting structure. The stoichiometry of the system is determined by the lattice we desire to assemble.

Interestingly, it is possible to devise a realization of the model using solely spherical particles interacting through isotropic potentials, thus avoiding the need to fabricate particles with complex shapes and interactions. This is shown in Fig. 1d, in which a cross-section of a cell containing a mixture of small spheres of diameter σ_0 that lie at the top of the cell and large spheres of diameter σ_2 located at the bottom of the cell. The non-additivity parameter σ_1 can be controlled by modifying the thickness of the cell h through the relationship

$$\frac{h}{\sigma_0} = \frac{1}{2}\left[1 + \frac{\sigma_2}{\sigma_0} + \sqrt{\left(\frac{\sigma_2}{\sigma_0} - \frac{\sigma_1}{\sigma_0}\right)\left(2 + \frac{\sigma_1}{\sigma_0} + \frac{\sigma_2}{\sigma_0}\right)}\right]. \quad (4)$$

As an example, in Fig. 1e we sketch the assembly of spheres that reproduces the lattice shown in panel (c).

Results and discussion

Standard Monte Carlo (MC) simulations based on the canonical ensemble (NVT simulations) in a square box of side L with periodic boundary conditions were carried out using the Metropolis algorithm. We used σ_0 and ε_0 as length and energy units, respectively, the reduced temperature $T^* = k_B T/\varepsilon_0$, where k_B is Boltzmann's constant, and the reduced number density $\rho^* = (N_M\sigma_1^2 + N_D\sigma_0^2)/L^2$, where N_i stands for the number of particles of species i.

Simulations were performed with $N \approx 1000$ particles, and control runs with $N \approx 5000$ particles to exclude finite size effects were also done. In all cases, the system is first disordered at high temperature and then brought from $T^* = 3.0$ to the final temperature $T^* = 0.01$ through an accurate annealing procedure with steps of 0.01. An equilibration cycle consisted, for each temperature, of at least 1×10^8 MC steps, each one representing one trial displacement of each particle, on average. At every simulation step a particle is picked at random and given a uniform random trial displacement within a radius of $0.1\sigma_0$. The range of the potential wells was $\lambda_i = 1.05\sigma_i$, with $i = 0, 2, 01$.

In the following we explore the parameter space set by the parameters σ_1/σ_0, σ_2/σ_0, ε_0, ε_2, and ε_{01}, and construct a number of different target structures. First, we consider the case in which each M-type particle is in contact with only two discs in order to form chains. We can achieve this by setting a small value of σ_1/σ_0. Three examples are displayed in Fig. 2. Panel (a) shows the result for $\sigma_1/\sigma_0 = 0.02$, $\sigma_2/\sigma_0 = 1.8$, and $\varepsilon_2 = 0$. The small value for σ_1/σ_0 is chosen so that M-type particles act as stickers between two discs. On the other hand, the value of σ_2/σ_0 is chosen so that only a small fraction of the discs protrudes from the cap of the M-type particles therefore forming effectively anisotropic particles with two interacting patches. The

Published on 28 November 2014. Downloaded by FAC DE QUIMICA on 03/03/2016 17:58:19.

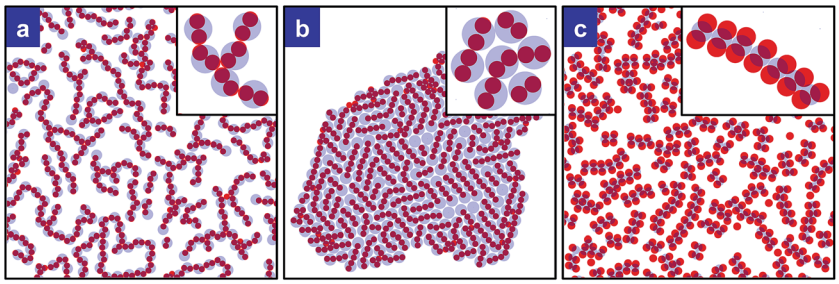

Fig. 2 Chains and stripes obtained with $n = 2$. (a) Polymer like structures obtained with $\sigma_1/\sigma_0 = 0.02$ and $\sigma_2/\sigma_0 = 1.8$. A few branching points are present as shown in the inset. (b) $\sigma_1/\sigma_0 = 0.02$ and $\sigma_2/\sigma_0 = 2$. (c) $\sigma_1/\sigma_0 = 0.02$ and $\sigma_2/\sigma_0 = 1.08$. The depths of the potential wells (ε_0, ε_2, ε_{01}) for each structure are (0.5, 0, 1.5), (0.5, 1, 1.5), and (0, 0.5, 1.5), respectively.

resulting patchy particles join to form flexible chains with a few branching points. Furthermore, by varying the values of σ_1/σ_0 and σ_2/σ_0, the persistence length of the chains can be controlled to certain extent. Panel (b) shows the result of using $\sigma_1/\sigma_0 = 0.02$, $\sigma_2/\sigma_0 = 2$ and $(\varepsilon_0, \varepsilon_2, \varepsilon_{01}) = (0.5, 1, 1.5)$. In this case, M-type particles form a triangular lattice to maximize their favorable contacts and the discs accommodate in domains of mostly parallel stripes, some of them with a few bends. Panel (c) shows the result when $\sigma_1/\sigma_0 = 0.02$, $\sigma_2/\sigma_0 = 1.08$, and $(\varepsilon_0, \varepsilon_2, \varepsilon_{01}) = (0, 0.5, 1.5)$.

Now we turn to the cases given by eqn (1), progressively increasing the value of n and using different choices for σ_2/σ_0 and the depth of the potential wells, ε_0, ε_2, and ε_{01}.

For $n = 3$, using eqn (1) and (2), a triangular lattice made of discs is intercalated with a honeycomb lattice made of M-type particles, as shown in Fig. 3a. Drawing lines joining each particle of the lattice with its nearest neighbors we observe that it can be characterized by a plane tiling of regular hexagons (inset). On the other hand, if eqn (3) is used, then a Kagomé lattice of discs is intercalated with a triangular lattice of M-type particles, as shown in Fig. 3b. In the Kagomé lattice each particle is in contact with four other particles of the same species. If we tessellate the Kagomé lattice by drawing lines between nearest neighbors, we observe that each vertex of the lattice is surrounded by two triangles and two hexagons (see the inset). In general, the vertex of a tiling made of regular polygons can be described as $(n_1.n_2.n_3\ldots)$ corresponding to the numbers of sides of the polygons listed in order. Using that notation, our lattice can be written as (3.6.3.6) and is also known as trihexagonal tiling and is an example of Archimedean tiling. Archimedean tilings are defined as regular patterns of polygonal tessellation of a plane by regular polygons where only one type of vertex is permitted in each tiling. The possibility of decorating patchy particles so that they self-assemble Archimedean tilings has been theoretically studied.[31] Such Archimedean tilings have also recently been self-assembled using enthalpically and entropically patchy polygons.[32] Notice that in this case not all M-type particles are equivalent since some of them are in contact with three discs while others, located at the pores of the Kagomé lattices, are not in contact with the discs but only with neighboring M-type particles. Kagomé lattices have been self-assembled using trijanus particles[13] and their stability in this case is favored by entropy.[24] However, in our model the relevant quantity is energy since the system is trying to minimize its interactions by maximizing the number of favorable contacts between particles.

Another interesting target structure with a great deal of technological potential is the twisted Kagomé lattice[16] since it is an arrangement that presents negative Poisson's ratio (auxetic behavior).[25] An auxetic material, when stretched in a particular direction, expands in an orthogonal direction. In the present model, twisted Kagomé lattices are obtained for intermediate

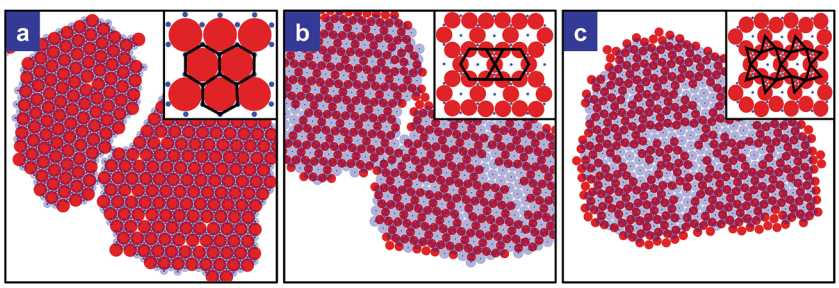

Fig. 3 Honeycomb, Kagomé, and twisted Kagomé tilings obtained with $n = 3$. (a) σ_1/σ_0 and σ_2/σ_0 as given by eqn (1) and (2), respectively. A triangular lattice of discs (red) is intercalated with a honeycomb lattice of M-type particles (blue). The inset shows the (6^3) motif of the regular M-type particle tiling. (b) σ_1/σ_0 and σ_2/σ_0 as given by eqn (1) and (3), respectively. A triangular lattice of M-type particles (blue) is intercalated with a Kagomé lattice of discs (red). The inset shows the (3.6.3.6) motif of the tiling of discs. (c) Twisted Kagomé lattice obtained with $\sigma_1/\sigma_0 \simeq 0.1547$, as given by eqn (1) and $\sigma_2/\sigma_0 = 1.1$. The inset shows two plaquettes of the lattice. The depths of the potential wells (ε_0, ε_2, ε_{01}) for each structure are (1, 2, 1), (1, 2, 1), and (0.7, 1, 1), respectively.

 This journal is © The Royal Society of Chemistry 2015

Published on 28 November 2014. Downloaded by FAC DE QUIMICA on 03/03/2016 17:58:19.

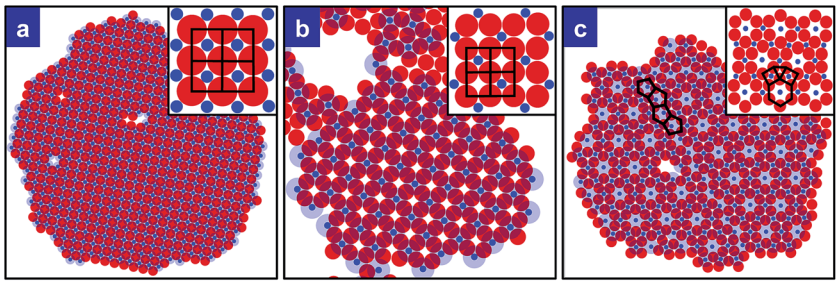

Fig. 4 Square and semi-regular rhombitrihexagonal tilings obtained with $n = 4$. (a) σ_1/σ_0 and σ_2/σ_0 as given by eqn (1) and (2), respectively. In this case a square lattice of discs (red) is intercalated with a square lattice of M-type particles (blue). (b) σ_1/σ_0 and σ_2/σ_0 as given by eqn (1) and (3). In this case a square lattice of discs (red) is intercalated with a square lattice of M-type particles (blue) rotated 45 degrees with respect to the first lattice. (c) Semi-regular rhombitrihexagonal tiling of discs (red) obtained with $\sigma_1/\sigma_0 = \sqrt{2} - 1$, as given by eqn (1), and $\sigma_2/\sigma_0 \simeq 1.37$. The lattice is intercalated with a triangular lattice of M-type particles (blue). A dislocation line in the lattice of discs formed by pentagons is highlighted with black lines. The inset shows the (3.4.6.4) vertex that decorates the Archimedean lattice of discs. The depths of the potential wells (ε_0, ε_2, ε_{01}) for each structure are (1, 1, 1), (1, 1, 1), and (0.5, 1.5, 1), respectively.

values of σ_2/σ_0 as shown in Fig. 3c, where the value $\sigma_2/\sigma_0 = 1.1$ is used. It has been shown that twisted Kagomé lattices can be obtained as a minimum energy configuration of patchy particles with five-patch particles, decorated with two A and three B patches, in which like patches attract each other, while unlike patches repel each other.[7] In contrast, in our model, the twisted Kagomé lattices are self-assembled using only isotropic interactions.

Examples of lattices obtained with $n = 4$ are shown in Fig. 4. Panel (a) shows a case using eqn (1) and (2). Two intercalated square lattices are formed. Panel (b) shows the structure obtained when using eqn (3). Two square lattices are formed but their principal axes are rotated 45 degrees with respect to each other, and a square lattice of voids is also apparent. Panel (c) shows a triangular lattice of M-type particles intercalated with a very open structure of discs. Lines connecting neighboring discs show that each vertex of the lattice is surrounded by a triangle, two squares and a hexagon [inset of Fig. 4 panel (c)] and can be written as (3.4.6.4). This lattice is known as semi-regular, rhombitrihexagonal tiling and is another example of Archimedean tiling (inset of Fig. 4c). Notice the interesting dislocation consisting of a chain of pentagons as it is highlighted by the black lines in Fig. 4c.

Fig. 5 shows a case obtained with $n = 4$. Eqn (1) gives $\sigma_1/\sigma_0 \simeq 0.4142$ and we have used $\sigma_2/\sigma_0 \simeq 1.366$ and $(\varepsilon_0, \varepsilon_2, \varepsilon_{01}) = (1, 1, 1)$. In panel (a) we observe that M-type particles form a regular

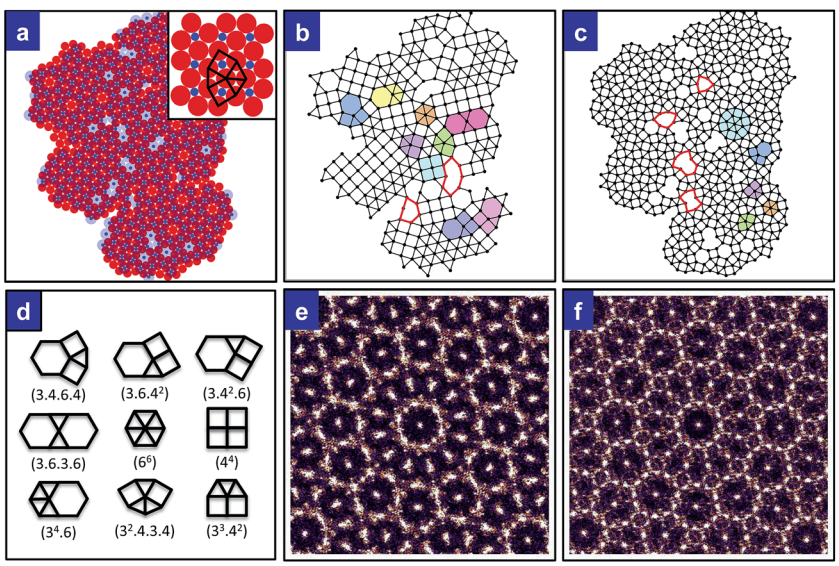

Fig. 5 Polycrystalline snub square obtained with $n = 4$. (a) Polycrystalline snub square lattice of discs (red) obtained with σ_1/σ_0, as given by eqn (1) and $\sigma_2/\sigma_0 \simeq 1.366$. For a given domain (see the inset), the lattice of discs is intercalated with a square lattice of M-type particles (blue). The inset shows the $(3^2.4.3.4)$ vertex that decorates the lattice of discs. (b) Square-triangular pattern corresponding to the M-type particles. The different vertices forming this pattern are highlighted with shadowed tiles. Red lines connect regions that cannot be joined by regular polygons. (c) Square-triangular pattern corresponding to the discs. The different vertices forming this pattern are highlighted with shadowed tiles. Red lines connect regions that cannot be joined by regular polygons. A dodecagonal motif typically found in quasicrystals is highlighted in cyan. (d) Summary of the types of vertices found in the patterns shown in panels (b) and (c). (e) and (f) are diffraction patterns of the lattice of M-type particles and of discs, respectively, showing twelve-fold symmetry. The depths of the potential wells (ε_0, ε_2, ε_{01}) are (1, 1, 1).

Published on 28 November 2014. Downloaded by FAC DE QUIMICA on 03/03/2016 17:58:19.

square lattice while each disc is in contact with five other discs and form a lattice of "tilted" squares. Drawing lines connecting neighboring discs we observe that each vertex of the lattice can be written as $(3^2.4.3.4.)$, a lattice also known as snub square tiling (see the inset of Fig. 5a). In panels (b) and (c) we show the structural motifs formed by joining with lines neighboring particles that constitute the M-type particle and disc lattices, respectively. Note the defects present in the lattices, basically, vacancies with different geometrical shapes. Defects ensure that the relative angles between the microcrystals forming the polycrystalline structure are not arbitrary. For example, panel (b) shows clearly that the relative angles between different snub square tilings are multiples of 60 degrees. The different vertices that decorate the lattice of M-type particles are highlighted with shaded plaquettes. Regions of the lattice that cannot be joined by regular polygons are highlighted with red lines. Fig. 5c shows that the structural motifs that decorate the lattice of discs are globally different from those corresponding to the M-type particles. However, the vertices that decorate the lattice are of the same type. Also, a dodecagonal pattern usually seen in quasicrystals is also highlighted. Red lines connect representative regions that cannot be joined by regular polygons. Fig. 5d summarizes the types of vertices found in both lattices. The presence of the defects is relevant as can be seen in the diffraction patterns [Fig. 5 panels (e) and (f)]. A snub square tiling would produce a diffraction pattern with square symmetry. However, the diffraction produced by the self-assembled structure shows a pattern consistent with a twelvefold symmetry.

Clearly, the case with $n = 5$ is particularly interesting since in this case the local symmetry is incompatible with crystalline order. This suggests the possibility to construct aperiodic structures with long-range order, that is, quasicrystals (or their approximants). Quasicrystalline heterostructures fabricated from dielectric materials with micrometer-scale features exhibit interesting and useful optical properties including large photonic bandgaps in two-dimensional systems.[26] Thus, they are an interesting case to self-assemble. As expected, it is possible to choose the geometrical parameters such that the resulting structure presents rotational symmetry consistent with a twelvefold-symmetric quasicrystal as shown in Fig. 6a. Careful examination of the structure shows a crystalline domain in the upper left quadrant of the structure. This crystalline region is highlighted in panel (b) where the structural motif of the lattice formed by M-type particles is drawn with black lines. Again, a $(3^2.4.3.4)$ snub square tiling is formed. Lines connecting neighboring M-type particles of the whole lattice show a square-triangular tiling (see Fig. 6c) whose vertices can be of three different types: $(3^2.4.3.4)$ is highlighted with green color, $(3^3.4^2)$ is marked in purple, and (3^6) in orange. A dodecagonal structural motif usually present in quasicrystals is shown in cyan color. It is known that patterns of squares and triangles tend to form twelvefold-symmetric quasicrystals.[33,34] Formation of the

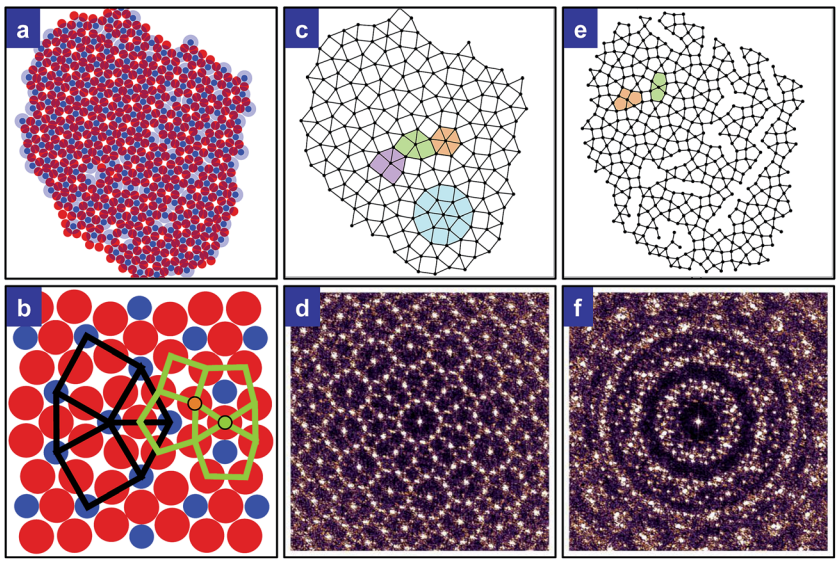

Fig. 6 Dodecagonal quasicrystal obtained with $n = 5$. Structure obtained with σ_1/σ_0, as given by eqn (1) and with $\sigma_2/\sigma_0 \simeq 1.72$. (a) In this case a dodecagonal quasicrystal of M-type particles (blue) is intercalated with a lattice of discs forming pentagons (red). The lattice of M-type particles shows a snub square crystal in the upper left quadrant. The rest of the structure has a symmetry consistent with a twelvefold symmetry. (b) Snub square section of the lattice, showing the $(3^2.4.3.4)$ motif (black lines). The lattice of discs presents two types of vertices, a (3.5.4.5) vertex (orange dot) and a (3.5.3.5) vertex (green dot). These motifs are not formed by regular polygons since the sum of their internal angles does not add to 360 degrees. Therefore, the polygons are slightly deformed (green lines). (c) Square-triangular pattern corresponding to the M-type particles. Three neighbor classification of σ (green), H (purple), and Z (orange) environments is shown. A dodecagonal motif typically found in quasicrystals is highlighted in cyan. (d) Diffraction pattern of the lattice formed by the M-type particles showing dodecagonal symmetry. (e) Pattern of non-regular triangles and pentagons corresponding to the discs. The two types of vertices are highlighted with orange (3.5.4.5) and green (3.5.3.5). Regions where defects are present cannot be covered by these motifs. (f) Diffraction pattern of the lattice of discs. The depths of the potential wells (ε_0, ε_2, ε_{01}) are (1, 1, 1).

 This journal is © The Royal Society of Chemistry 2015

Published on 28 November 2014. Downloaded by FAC DE QUIMICA on 03/03/2016 17:58:19.

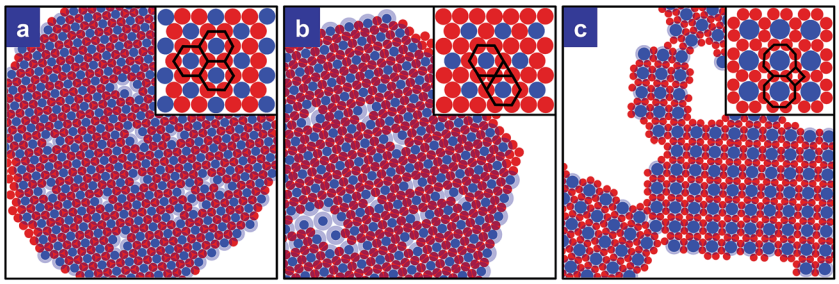

Fig. 7 Honeycomb, Kagomé, and truncated square tilings obtained with $n = 6$ and 8. (a) Honeycomb lattice of discs (red) obtained with $n = 6$, σ_1/σ_0, and σ_2/σ_0 as given by eqn (1) and (2), respectively. (b) $n = 6$, σ_1/σ_0, and σ_2/σ_0 as given by eqn (1) and (3), respectively. A triangular lattice of M-type particles (blue) is intercalated with a Kagomé lattice of discs (red). The inset shows the (3.6.3.6) motif of the Kagomé tiling. (c) $n = 8$, σ_1/σ_0, and σ_2/σ_0 as given by eqn (1) and (2), respectively. In this case a square lattice of M-type particles (blue) is intercalated with a truncated square tiling of discs (red). The inset shows the (4.8^2) motif. The depth of the potential wells (ε_0, ε_2, ε_{01}) are (1, 1, 1) in all cases.

dodecagonal quasicrystal in a square-triangle lattice requires that the total tiling area occupied by squares be equal to that occupied by triangles,[34] that is, $N_3/N_4 = 4/\sqrt{3} \simeq 2.31$, a value that closely corresponds to the simulation results. A confirmation of this fact is the diffraction pattern of the M-type particle lattice which is consistent with a dodecagonal quasicrystal, as shown in Fig. 6d. Panel (e) shows the polygonal tiling corresponding to the positions of the discs. Two structural motifs are present, a (3.5.3.5) vertex shown in green and a (3.5.4.5) vertex shown in orange [see also panel (b)]. However, these motifs are not made of regular polygons since the sum of their internal angles do not add to 360 degrees. Actually, a regular n-gon has an internal angle $(1 - 2/n)$ of 180 degrees and there is a limited number of combinations whose internal angles add to 360 degrees. Thus, the structural motifs of the lattice of discs are made of deformed polygons, which are allowed thanks to the flexibility produced by the width of the potential wells. The regions where the defects are present cannot be tessellated by these nearly regular polygons. The corresponding diffraction pattern is shown in panel (f).

Alternative procedures to self-assemble quasicrystals and their approximants have been proposed. They are based on particle functionalization with mobile surface entities and shape polydispersity[35] or with the use of five and seven patched particles.[36] In contrast, our method uses only isotropic interactions. A family of quasicrystals have also been found using hard core-square shoulder interparticle potentials in ref. 37.

The case with $n = 6$ provides an alternative procedure to construct the honeycomb and Kagomé lattices. The first case, obtained using eqn (1) and (2), is shown in Fig. 7a. When using eqn (3) a triangular lattice of M-type particles intercalated with a Kagomé lattice of discs is obtained [Fig. 7b]. We have not obtained regular lattices or other recognizable structures formed with $n = 7$.

Finally, the structure formed with $n = 8$ and using eqn (1) and (3) is shown in Fig. 7c. The truncated square tiling with vertex (4.8^2) is shown in the inset.

Our results are summarized in the zero temperature phase diagram shown in Fig. 8. The green and red lines represent eqn (2) and (3), respectively. The energies used to obtain any given structure are indicated by the triplets (ε_0, ε_2, ε_{01}). Clearly, for the same set of σ_1/σ_0 and σ_2/σ_0, other structures could be obtained by using different choices for the energies. Above the straight-line $\sigma_2/\sigma_0 = 2 + \sigma_1/\sigma_0$ and for the right stoichiometry, the system consists of a fluid (if $\varepsilon_2 = 0$ and for low concentrations) or a crystal (if $\varepsilon_2 \neq 0$ or for large concentrations) of meta-particles composed of an M-type particle surrounded by n discs. The large value of σ_2 prevents the interaction of discs belonging to different meta-particles. Therefore, the meta-particles interact as isotropic discs of diameter σ_2. On the other hand, for values of σ_2/σ_0 below that given by eqn (2), the meta-particle interactions have n-gonal symmetry, as represented by the drawings in Fig. 8.

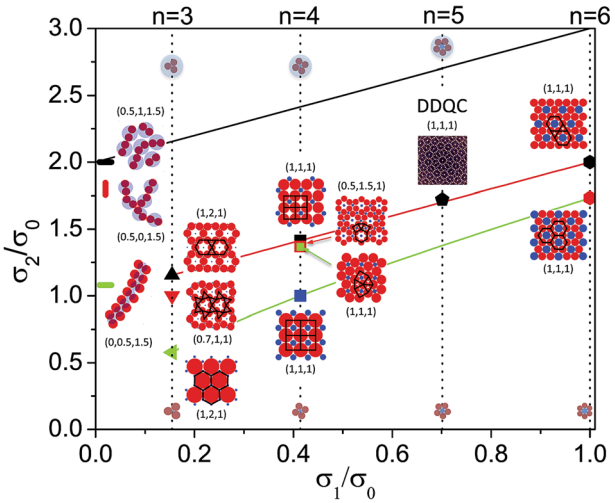

Fig. 8 Phase diagram. Summary of the self-assembled structures. The green and red lines are the values of σ_2/σ_0 given by eqn (2) and (3), respectively. The black straight line is $\sigma_2/\sigma_0 = 2 + \sigma_1/\sigma_0$. Above this value, the system consists of a fluid (if $\varepsilon_2 = 0$ and for low concentrations) or a crystal (if $\varepsilon_2 \neq 0$ or for large concentrations) of meta-particles. Symbols correspond to the structures built in this study and the triplets (ε_0, ε_2, ε_{01}) above or below each inset correspond to the energies used to obtain the corresponding lattice. The dodecagonal quasicrystal (DDQC) is represented by its diffraction pattern.

Published on 28 November 2014. Downloaded by FAC DE QUIMICA on 03/03/2016 17:58:19.

Conclusions

In conclusion, we have presented a model that is able to generate a large variety of pre-programmed structures. We emphasize the simplicity of the interactions which are isotropic, and the relative ease with which we get complex structures by controlling a small number of geometrical and energetic parameters. Furthermore, our two species model can be straightforwardly generalized to three or more species to construct more complex lattices, including, for example, self-similar structures. Let us stress that the simplicity of the model, the fact that it can be implemented using exclusively spherical particles interacting isotropically and the large variety of methods to produce short range attractions, including the use of depletion[38] or DNA-mediated[39] interactions, make the feasibility to put into practice the present model very realistic. Finally, we suggest that if the experiments are performed using chemically or temperature sensitive particles that can change size, then the system could potentially switch smoothly between different lattices, something that would be difficult to achieve with other systems.

Acknowledgements

We are grateful to Zorana Zeravcic for useful comments. This work was supported in part by grant DGAPA IN-110613. DSB acknowledges financial support from CONACyT through scholarship Num. 207347.

References

1 H. K. Choi, S. H. Im and O. O. Park, Fabrication of unconventional colloidal self-assembled structures, *Langmuir*, 2010, **26**, 12500–12504.
2 B. A. Grzybowski, C. E. Wilmer, J. Kim, K. P. Browne and K. J. M. Bishop, Self-assembly: from crystals to cells, *Soft Matter*, 2009, **5**, 1110–1128.
3 S. C. Glotzer and M. J. Solomon, Anisotropy of building blocks and their assembly into complex structures, *Nat. Mater.*, 2007, **6**, 557–562.
4 S. Sacanna and D. J. Pine, Shape-anisotropic colloids: Building blocks for complex assemblies, *Curr. Opin. Colloid Interface Sci.*, 2011, **16**, 96–105.
5 K. J. Lee, J. Yoon and J. Lahann, Recent advances with anisotropic particles, *Curr. Opin. Colloid Interface Sci.*, 2011, **16**, 195–202.
6 Z. Zhang and S. C. Glotzer, Self-Assembly of Patchy Particles, *Nano Lett.*, 2004, **4**, 1407–1413.
7 G. Doppelbauer, E. Bianchi and G. Kahl, Self-assembly scenarios of patchy colloidal particles in two dimensions, *J. Phys.: Condens. Matter*, 2010, **22**, 104105.
8 A. B. Pawar and I. Kretzschmar, Fabrication, Assembly, and Application of Patchy Particles, *Macromol. Rapid Commun.*, 2010, **31**, 150–168.
9 A. G. Vanakaras, Self-Organization and Pattern Formation of Janus Particles in Two Dimensions by Computer Simulations, *Langmuir*, 2006, **22**, 88–93.
10 S. Jiang, *et al.* Janus Particle Synthesis and Assembly, *Adv. Mater.*, 2010, **22**, 1060–1071.
11 F. Romano and F. Sciortino, Two dimensional assembly of triblock Janus particles into crystal phases in the two bond per patch limit, *Soft Matter*, 2011, **7**, 5799–5804.
12 Z.-W. Li, Z.-Y. Lu and Z.-Y. Sun, Soft Janus particles: ideal building blocks for template-free fabrication of two-dimensional exotic nanostructures, *Soft Matter*, 2014, **10**, 5472–5477.
13 Q. Chen, S. C. Bae and S. Granick, Directed self-assembly of a colloidal Kagomé lattice, *Nature*, 2011, **469**, 381–384.
14 E. A. Jagla, Phase behavior of a system of particles with core collapse, *Phys. Rev. E: Stat. Phys., Plasmas, Fluids, Relat. Interdiscip. Top.*, 1998, **58**, 1478–1486.
15 G. Malescio and G. Pellicane, Stripe phases from isotropic repulsive interactions, *Nat. Mater.*, 2003, **2**, 97–100.
16 S. Torquato, Inverse optimization techniques for targeted self-assembly, *Soft Matter*, 2009, **5**, 1157–1173.
17 R. D. Batten, D. A. Huse, F. H. Stillinger and S. Torquato, Novel ground-state crystals with controlled vacancy concentrations: From kagomé to honeycomb to stripes, *Soft Matter*, 2011, **7**, 6194–6204.
18 C. Tang, E. M. Lennon, G. H. Fredrickson, E. J. Kramer and C. J. Hawker, Evolution of Block Copolymer Lithography to Highly Ordered Square Arrays, *Science*, 2008, **322**, 429–432.
19 D. V. Talapin, *et al.* Quasicrystalline order in self-assembled binary nanoparticle superlattices, *Nature*, 2009, **461**, 964–967.
20 K. S. Khalil, *et al.* Binary Colloidal Structures Assembled through Ising Interactions, *Nat. Commun.*, 2012, **3**, 794.
21 M. Grünwald and P. L. Geissler, Patterns without Patches: Hierarchical Self-Assembly of Complex Structures from Simple Building Blocks, *ACS Nano*, 2014, **8**, 5891–5897.
22 I. Syôzi, Statistics of Kagomé Lattice, *Prog. Theor. Phys.*, 1951, **6**, 306–308.
23 X. Li, J. Zhou, Q. Wang, X. Chen, Y. Kawazoe and P. Jena, Magnetism of two-dimensional triangular nanoflake-based kagomé lattices, *New J. Phys.*, 2012, **14**, 033043.
24 X. Mao, Q. Chen and S. Granick, Entropy favours open colloidal lattices, *Nat. Mater.*, 2013, **12**, 217–222.
25 K. Sun, A. Souslov, X. Mao and T. C. Lubensky, Surface phonons, elastic response, and conformal invariance in twisted kagomé lattices, *Proc. Natl. Acad. Sci. U. S. A.*, 2012, **109**, 12369–12374.
26 Y. Roichman and D. G. Grier, Holographic assembly of quasicrystalline photonic heterostructures, *Opt. Express*, 2005, **13**, 5434–5439.
27 D. Coslovich and G. Pastore, Dynamics and energy landscape in a tetrahedral network glass-former: direct comparison with models of fragile liquids, *J. Phys.: Condens. Matter*, 2009, **21**, 285107.
28 N. Osterman, D. Babič, I. Poberaj, J. Dobnikar and P. Ziherl, Observation of condensed phases of quasiplanar core-softened colloids, *Phys. Rev. Lett.*, 2007, **99**, 248301.
29 P. Hopkins and M. Schmidt, Binary non-additive hard sphere mixtures: fluid demixing, asymptotic decay of

 This journal is © The Royal Society of Chemistry 2015

Published on 28 November 2014. Downloaded by FAC DE QUIMICA on 03/03/2016 17:58:19.

correlations and free fluid interfaces, *J. Phys.: Condens. Matter*, 2010, **22**, 325108.
30 R. Faller and T. L. Kuhl, Modeling the binding of cholera-toxin to a lipid membrane by a non-additive two-dimensional hard disk model, *Soft Mater.*, 2003, **1**, 343–352.
31 M. Antlanger, G. Doppelbauer and G. Kahl, On the stability of Archimedean tilings formed by patchy particles, *J. Phys.: Condens. Matter*, 2011, **23**, 404206.
32 J. A. Millan, D. Ortiz, G. van Anders and S. C. Glotzer, Self-Assembly of Archimedean Tilings with Enthalpically and Entropically Patchy Polygons, *ACS Nano*, 2014, **8**, 2918–2928.
33 M. Oxborrow and C. L. Henley, Random square-triangle tilings: A model for twelvefold-symmetric quasicrystals, *Phys. Rev. B: Condens. Matter Mater. Phys.*, 1993, **48**, 6966–6998.
34 M. Widom, Bethe ansatz solution of the square-triangle random tiling model, *Phys. Rev. Lett.*, 1993, **70**, 2094–2097.
35 C. R. Iacovella, A. S. Keys and S. C. Glotzer, Self-assembly of soft-matter quasicrystals and their approximants, *Proc. Natl. Acad. Sci. U. S. A.*, 2011, **108**, 20935–20940.
36 M. N. van der Linden, J. P. K. Doye and A. A. Louis, Formation of dodecagonal quasicrystals in two-dimensional systems of patchy particles, *J. Chem. Phys.*, 2012, **136**, 054904.
37 T. Dotera, T. Oshihiro and P. Ziherl, Mosaic two-lengthscale quasicrystals, *Nature*, 2014, **506**, 208–211.
38 H. N. W. Lekkerkerker and R. Tuinier, *Colloids and the Depletion Interaction*, Springer, Heidelberg, 2011.
39 A. J. Kim, P. L. Biancaniello and J. C. Crocker, Engineering DNA-Mediated Colloidal Crystallization, *Langmuir*, 2006, **22**, 1991–2001.